

Article

Plasma Spheroidisation of Irregular Ti6Al4V Powder for Powder Bed Fusion

Nthateng Nkhasi ^{1,*}, Willie du Preez ²  and Hertzog Bissett ³ 

¹ Department of Mechanical and Mechatronics Engineering, Central University of Technology, Bloemfontein 9301, Free State, South Africa

² Centre for Rapid Prototyping and Manufacturing, Faculty of Engineering, Built Environment and Information Technology, Central University of Technology, Bloemfontein 9301, Free State, South Africa; wdupreez@cut.ac.za

³ Applied Chemistry, South African Nuclear Energy Corporation SOC Ltd. (Necsa), Pretoria 0001, Gauteng, South Africa; hertzog.bissett@necsa.co.za

* Correspondence: nthatengnp@gmail.com

Abstract: Metal powders suitable for use in powder bed additive manufacturing processes should ideally be spherical, dense, chemically pure and of a specified particle size distribution. Ti6Al4V is commonly used in the aerospace, medical and automotive industries due to its high strength-to-weight ratio and excellent corrosion resistance properties. Interstitial impurities in titanium alloys have an impact upon mechanical properties, particularly oxygen, nitrogen, hydrogen and carbon. The plasma spheroidisation process can be used to spheroidise metal powder consisting of irregularly shaped particles. In this study, the plasma spheroidisation of metal powder was performed on Ti6Al4V powder consisting of irregularly shaped particles. The properties of the powder relevant for powder bed fusion that were determined included the particle size distribution, morphology, particle porosity and chemical composition. Conclusions were drawn regarding the viability of using this process to produce powder suitable for additive manufacturing.

Keywords: plasma spheroidisation; additive manufacturing; Ti6Al4V powder; powder bed fusion



Citation: Nkhasi, N.; du Preez, W.; Bissett, H. Plasma Spheroidisation of Irregular Ti6Al4V Powder for Powder Bed Fusion. *Metals* **2021**, *11*, 1763. <https://doi.org/10.3390/met11111763>

Academic Editors: Marco Mandolini, Paolo Cicconi and Patrick Pradel

Received: 3 September 2021

Accepted: 28 October 2021

Published: 2 November 2021

Publisher's Note: MDPI stays neutral with regard to jurisdictional claims in published maps and institutional affiliations.



Copyright: © 2021 by the authors. Licensee MDPI, Basel, Switzerland. This article is an open access article distributed under the terms and conditions of the Creative Commons Attribution (CC BY) license (<https://creativecommons.org/licenses/by/4.0/>).

1. Introduction

South Africa has a vision to raise its profile on the global business stage by adding value to its titanium-bearing mineral resource through turning it into metal powder that would be suitable for additive manufacturing (AM). In 2020, South Africa was rated the second largest mining producer of ilmenite (1000 t) and the third largest mining producer of rutile (100 t) in the world [1]. In South Africa, the Council for Scientific and Industrial Research (CSIR) built a pilot plant that produces commercially pure titanium powder [2]. The titanium powder is produced in this plant through the continuous stepwise metallothermic reduction of titanium tetrachloride in a molten salt medium. These titanium powders produced at the CSIR are intended to be used in various downstream manufacturing processes, such as AM, powder metallurgy and investment casting. However, the titanium metal powder produced through the CSIR-Ti process is either spongy or crystalline, depending on the process parameters [3]. For use in powder bed fusion (PBF), the metal powder should ideally be spherical, dense and chemically pure. An irregularly shaped particle is less desirable for PBF processes, because it increases the flow time and could reduce the packing density [4]. Powder consisting of spherical particles is usually produced by atomisation methods or plasma spheroidisation (PS) [5].

Titanium alloys primarily stand out due to high specific strength and excellent corrosion resistance. This also explains their preferential use in the aerospace sector, the chemical industry, medical engineering and the leisure sector [5]. Titanium and its alloys are well-established for their combination of relatively high strengths, low densities, and

excellent corrosion resistance [6,7]. Yield strengths are in a range from 480 MPa for some grades of commercial titanium to approximately 1100 MPa for structural alloys. Added to their static strength advantage is the fact that titanium alloys have a much better fatigue strength than the other lightweight alloys, such as those of aluminium and magnesium [8]. Titanium can be obtained in several different grades, and pure titanium is not as formidable as the different titanium alloys. The titanium alloy (Ti6Al4V) is the most extensively used. It has a credible machinability and excellent mechanical properties [9]. For various weight reduction applications in aerospace, automotive and marine equipment, the alloy has the best overall performance. It is also known to have various applications in medicine. The biocompatibility of Ti6Al4V is exceptional, especially when the requirement is to have direct contact with tissue or bone [10].

Plasmas are categorised as cold or thermal plasmas, based on the degree of ionisation as well as the relative temperatures and densities of the electrons, ions and neutrons in the plasma. Typical examples of cold plasmas include fluorescent lamps and glow discharges, and examples of thermal plasmas are direct current arc discharges and inductively coupled radio-frequency (RF) induction plasmas. Inductively coupled RF induction plasmas are the preferred choice for the spheroidisation of powder consisting of irregularly shaped particles. This is due to its high purity process, since there is no direct contact of any electrodes with the materials. It supports a wide range of operating conditions with oxidising, reducing and inert gases, and it provides a better purification process as a result of impurities evaporation at high temperature [11,12].

Vert et al. found that high-performance Ti6Al4V powder for AM can be achieved using an inductively coupled plasma (ICP) process [13]. High-performance Ti6Al4V powders are those without any satellites and are spherical with an improved packing density, a narrow particle size distribution (PSD) of 15–45 μm , a flowability of 27 s/50 g, an internal particle structure free of pores and a chemical composition complying with Grade 23 specification [13]. Zi et al. also stated that ICP is suitable for preparing spherical powders with both the apparent density and flowability of the tungsten powder improving from 5.99 to 10.81 g/cm^3 and from 12.7 s/50 g to 5.46 s/50 g, respectively, with a decrease in the feeding rate [14].

Bissett et al. conducted a study focused in the PS of irregularly shaped pure titanium metal powder while investigating the capabilities of a 15 kW Tekna plasma system that was purchased by the South African Nuclear Energy Corporation (Necsa) in 2016 [15]. The irregularly shaped titanium particles were spheroidised in the plasma system at various plasma operating conditions. Subsequently, the spheroidised powder was characterised in terms of morphology, density and flowability. From the experimental results, it was generally concluded that titanium particles that are highly spherical with increased density and improved flow are produced by thermal plasma treatment from irregularly shaped titanium particles under argon thermal plasma in the Tekna plasma system. Therefore, this system can be used for the spheroidisation of other metal and alloy powders [15]. Sheng et al. prepared spherical Ti6Al4V powder using an RF plasma from irregular Ti6Al4V powder as a feedstock [16]. The experimental results showed that spherical powder with smooth surfaces and favourable dispersion were obtained. Furthermore, the spheroidisation efficiency of the spherical powders was almost 100% [16].

Wei et al. conducted characterisation on Ti6Al4V powder that was spheroidised using an ICP [17]. They found that the spherical powder had smooth surfaces, a narrow PSD and favourable dispersion, as well as nearly 100% degree of sphericity. Furthermore, the conditioned density, dynamics of flowability, compressibility, permeability and shear performance of the spheroidised powder greatly improved [17].

Xie et al. conducted a comparative investigation into Ti6Al4V powders produced by electrode induction melting gas atomization (EIGA), PS and plasma atomisation (PA) [18]. PA powder has the fewest satellite spheres followed by EIGA and PREP Ti6Al4V powders. Li et al. fabricated spherical Ti6Al4V powder for AM by RF PS and deoxide using calcium [19]. They found that the appropriate feeding rate for higher spheroidisation ratios

and lower mass loss ratios is 140 g/min and the oxygen content of Ti6Al4V powder can be reduced to 1240 ppm deoxidation without phase transformation [18].

Chong et al. used ICP to spheroidise Ti6Al4V powder [20]. The spheroidisation ratio as high as 99% was reached, when the position of the inlet nozzle was 12.5 cm, the chamber pressure was 101.36 kPa, the powder feeding rate was 1.742 g/min, the plasma plate power was 27.2 kW and the PSD of raw particles was around 38–63 μm [20]. Yang et al. spheroidised polygonal TiH₂ powders, prepared by hydrogenation and a milling process with Ti scraps in an Ar plasma state [21]. Consequently, polygonal TiH₂ powders were successfully converted into spherical Ti powders by plasma treatment. It was found that the size of the powders also decreased from 30 to 21 μm by means of evaporation at the powder surface during the plasma treatment. Contaminants, such as Fe, Cr and Ni in the powders, were diminished owing to the surface evaporation and the emission of corresponding vapors during the plasma treatment [21].

From the literature, it can be concluded that different researchers spheroidise different feedstocks using ICP. In this study, the plasma spheroidisation process was used to treat the Ti6Al4V powder produced using a high-energy ball milling process at the CSIR [22]. The properties of the spheroidised powder were compared to those of commercial powder normally used for PBF. It was expected that the results of this study would confirm the viability of spheroidising CSIR Ti6Al4V powder on the industrial scale through an ICP system.

2. Materials and Methods

2.1. PS Process

Ti-6Al-4V powder produced using high-energy ball milling process [22] supplied by the CSIR was used as a feedstock. The spheroidisation of these irregularly shaped powder particles was performed using a 15 kW Tekna ICP system at Necsa. The system consisted of an RF generator, with a downward plasma torch placed on top of a water-cooled quenching stainless steel chamber, power supply unit, a cylindrical reactor, a vibrating feeding system, a powder collector, a gas delivery system and an off-gas exhaust system, as shown in Figure 1. The plasma torch includes three main parts, namely a four-turn induction coil cooled by water, an injection probe also cooled by water and a confinement tube. A vacuum system is connected to the reactor, so that it can reduce the pressure in order to facilitate the initiation of the plasma flame. A cyclone is used to separate the fine particles from the spheroidised particles using a centrifugal force.

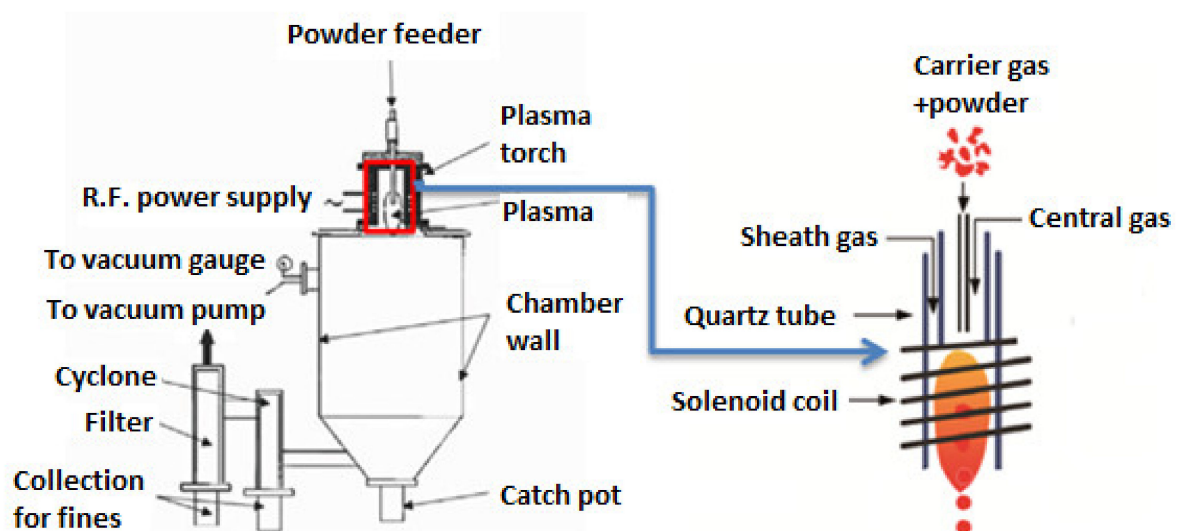


Figure 1. Schematic diagram of a plasma torch, adapted from [23].

The ICP can use three different gases, namely argon, hydrogen and helium. In most instances, argon and/or a mixture of argon and hydrogen or argon and helium can be used during spheroidisation process [23]. These gases flow into three concentric tubes, which are assembled in what is commonly referred to as a plasma torch. The flowing gas in the outer tube is normally referred to as the sheath gas. It is used mainly for two reasons, i.e., to ensure that the high temperature of the plasma does not melt the torch, thus preventing thermal damage to the side wall of the torch, and to give the plasma its distinct shape. The gas flowing in the central tube is referred to as the plasma gas and is the gas that is ionised to form a plasma. Subsequently, the gas flowing in the innermost ring is called the carrier gas and is used to punch the plasma whilst carrying a particulate form of the sample to be spheroidised.

The spheroidisation of the powder was performed under atmospheric pressure at a frequency of 3 MHz, and argon gas was used as a plasma-forming gas, a sheath gas and a carrier gas. The plasma parameters used for the spheroidisation of the irregularly shaped powder are outlined in Table 1. A powder size fraction of <45 µm was used as a feed material.

Table 1. Process parameters used for the plasma spheroidisation of Ti6Al4V powder.

Plasma Plate Power (kW)	11–13
Feed Rate (kg/h)	1
Carrier Gas Flowrate (slpm)	2
Plasma Gas Flowrate (slpm)	10
Sheath Gas Flowrate (slpm)	40
Particle Size Range (µm)	<45

The vibrating feeding system fed the powder at a controlled feed rate axially into the plasma flame with the assistance of a carrier gas, once the system reached the steady state.

Due to the extremely high temperature of the plasma torch, the powder was rapidly heated and completely melted inside the plasma and then immediately solidified, after the plasma exited. As the molten particles passed through the quenching chamber, they were condensed under the effect of surface tension and became spherical particles. The plasma gases and any vapours or fine powder were directed towards a sintered metal filter. From the filter, the gases were pumped into the exhaust system by a vacuum pump. When all the metal powders were spheroidised, the plasma system was allowed to cool and the powder was passivated to ensure safe removal. The resulting spherical powder particles were collected at the catch pot. The spherical powder was then cleaned to remove any fines that were present.

2.2. Characterisation of the Spheroidised Powder

The analysis techniques used for the characterisation of the Ti6Al4V powder samples complied with the international standards specified in the ASTM F3049-14 standard guide [24]. The particle morphology refers to the shape, size and surface roughness of the particle. In metal AM, the particle morphology is an essential property that determines the powder performance and thus impacts the final part properties. The morphology of the spheroidised powder was determined using a high-resolution JEOL JSM-6510 scanning electron microscope with an energy dispersive X-ray spectrometer (JEOL, Peabody, MA, USA). The powder samples were carefully mounted on a double carbon tape, and all loose powder particles were gently removed before introducing a sample holder with powder into the vacuum chamber of the scanning electron microscope. Images generated from the sample were displayed in the secondary electron (SE) mode, where low-energy electrons scattered by the particle surfaces form high-resolution images of surface topography. This mode clearly provided the morphology and the surface appearance of the powder. All the micrographs were taken in the SE mode, at an accelerating voltage of 20 kV and a working distance of 10 mm under vacuum conditions.

Manufacturing a part with an acceptable packing density and a smooth surface finish through PBF fundamentally depends on the PSD. The Saturn DigiSizer II instrument (Micromeritics Instruments, Norcross, GA, USA) was used to determine the PSD of the spheroidised powder, and the powder was tested three times with an equal powder mass to determine the average PSD, median particle sizes and the standard deviations. This laser diffraction technique can detect and measure the angular distribution of scattered light produced, as a laser beam passes through the dispersed particles. In a complex sample containing particles of different sizes, light diffraction results in specific diffraction patterns. These patterns are analysed to find the exact PSD.

The elemental composition of the Ti6Al4V powder was determined using a Spectro Arcos model inductively coupled plasma-optical emission spectroscopy (ICP-OES) instrument, (SPECTRO Analytical Instruments GmbH, Kleve, Germany). This technique uses the optical emission spectra of a sample to identify and quantify the elements present. ICP-OES was performed on the different samples. A powder sample (0.25 g) was dissolved in concentrated hydrofluoric acid and diluted with demineralised water. The mixture was then fed into a plasma where the atomisation and ionisation of powder took place. Subsequently, the constituent elements were then identified by their characteristic emission lines and quantified by the intensity of the same lines.

Oxygen and nitrogen concentrations strongly influence the properties of Ti6Al4V powder. Hence, a reliable and precise measurement of these elements is an important part of the quality control process. A Eltra combustion analyser (Eltra Elemental Analyzers, Haan, Germany), was used to determine the oxygen and nitrogen contents in the spheroidised Ti6Al4V powder. It uses the inert gas fusion technique for the elemental analysis of inorganic sample materials. For better reliability, a LECO ONH836 inert gas fusion analyser, LECO Europe B.V., Geleen, Netherlands, was also used to determine the oxygen, nitrogen and hydrogen contents of the spheroidised powder.

Although there is some overlap between techniques in terms of properties determined, this overlap serves to better compare the instruments and together they give a complete picture of the size, shape and composition of the metal powders.

3. Results and Discussion

An SEM micrograph and an EDS spectrum of the as-received powder from CSIR are shown in Figure 2. From the micrographs, it is clear that the powder consisted of various particles sizes and morphologies. The particles had rough needle-like structures and porous irregular structures with jagged surface features. The EDS analysis results in wt % confirmed the chemical composition of the Ti6Al4V powder.

The characteristics of the Ti6Al4V powder after spheroidisation are presented in terms of particle morphology, size distribution, porosity and chemical composition based on the analytical techniques used.

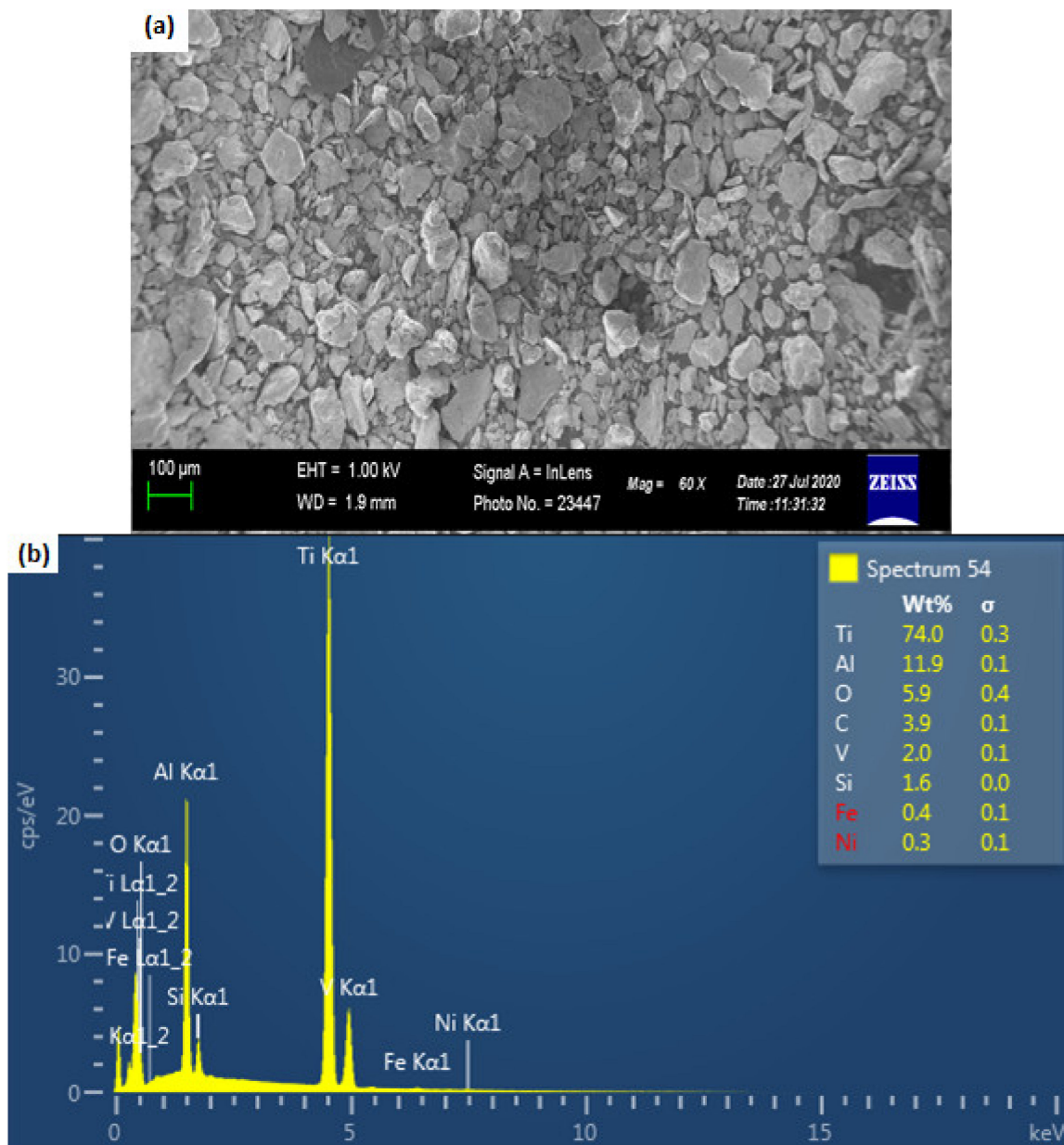


Figure 2. Scanning electron microscope (SEM) micrograph (a) and energy dispersive X-ray spectrometer (EDS) results (b) of the as-received powder from the Council for Scientific and Industrial Research (CSIR).

3.1. Particle Morphology

The shapes of individual particles play a role in the interactions with other particles within a powder. Each particle of powder interacts with the particles surrounding it, exerting forces on one another. The cumulative result of these forces causes powder to behave differently to just one individual particle. The SEM micrographs displayed the shapes, sizes and surface features of various particles of the spheroidised powder, both qualitatively and quantitatively, as shown in Figure 3. From the micrograph at a magnification of $180\times$, shown in Figure 3a, the particles appeared to be spherical with no satellites. During the PS, the as-received powder passed through a high-temperature plasma region, rapidly absorbed the heat and melted. The particles melted completely and were drawn into spherical shapes by surface tension. This significantly increased the flowability of the powder.

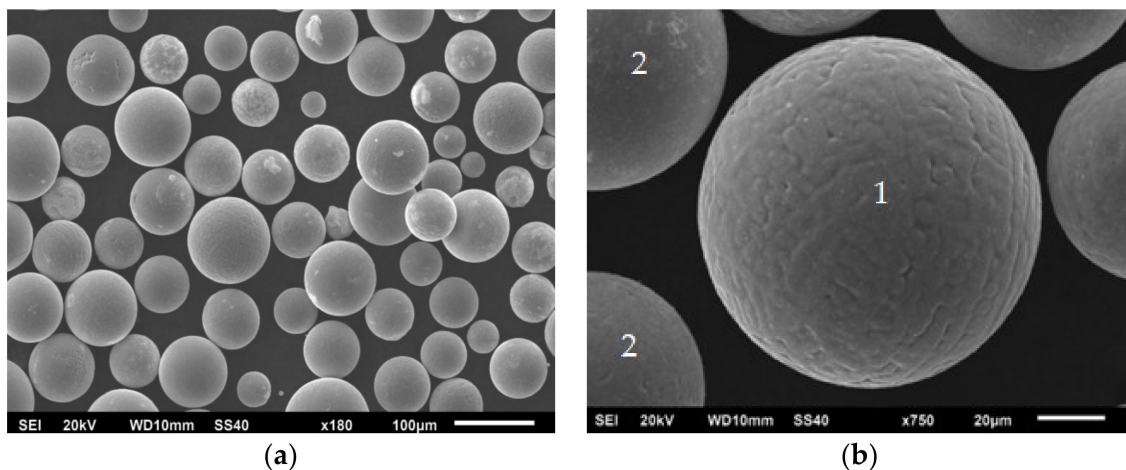


Figure 3. SEM secondary-electron images displaying the particle shape of the spheroidised powder (a) and the particle surface (coarse (labelled 1) and smooth (labelled 2) surface morphologies) (b).

The dominant presence of spherical particles complies with the need for good flowability, resulting in smoother layers, improved packing density, increased heat conduction in the PBF powder bed and an enhanced melting profile. The absence of satellites due to using an ICP system for powder spheroidisation is an additional benefit. These spherical particles revealed by the micrographs clearly confirmed that the effective spheroidisation of the powder occurred during the plasma treatment. Moreover, there was noticeable white debris on the surfaces of some particles, as can be seen in Figure 3a. This could be due to the partial vaporisation of the particles during its plasma heating and melting, followed by the condensation of the formed vapours on the surface of the particles in the cooling phase of their trajectory [13].

Particles will always have imperfections on their surfaces, referred to as surface roughness. The extent of this roughness influences how closely packed particles can be to one another; a rougher particle will be packed less densely than a smoother one. At a magnification of $750\times$ (Figure 3b), the surface morphology of the particles was clearly portrayed. Both the coarse (labelled 1) and smooth (labelled 2) surface morphologies can be observed, as shown in Figure 3b. The difference between the surface morphologies could be related to the cooling rate and the particle size of the molten droplet. Larger particles generally reveal more coarse surface features because of the relatively lower cooling rate, which gives rise to a longer solidification time, while finer particles tend to show a smoother surface morphology [25].

3.2. Particle Porosity

The spheroidisation of the powder was analysed through micro-CT scanning to determine the powder particle porosity. The resultant slice images showed the internal porosity and details of the morphology. The internal porosity was detected as black areas inside grey particles, as shown in Figure 4. However, although internal pores could be detected in the particles of the spheroidised powder, they were not easily noticeable due to the even small particles of the spheroidised powder. This was due to the fact that the powder totally melted during plasma treatment. In PBF, the presence of excessive amounts of large pores or pores with entrapped gas can negatively affect material properties of parts produced through this process. Moreover, there were only a few noticeable pores on the surface of powder particles, with an isolated example circled in red in Figure 5 as determined by SEM.

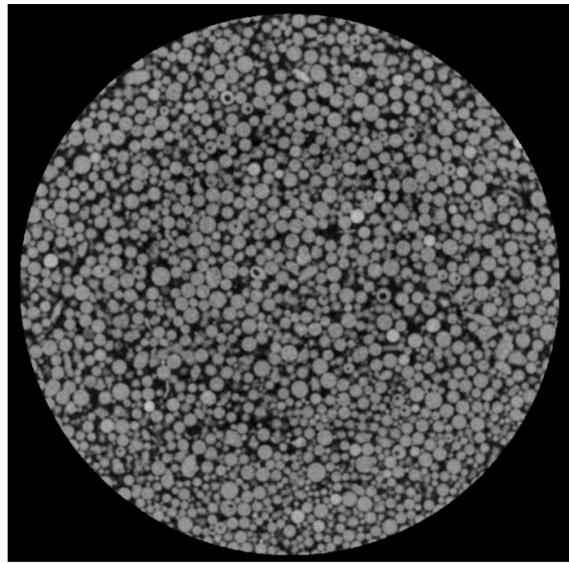


Figure 4. Slice image with micro-CT scanning showing indicating pores in black inside the grey particles for the spheroidise powder.

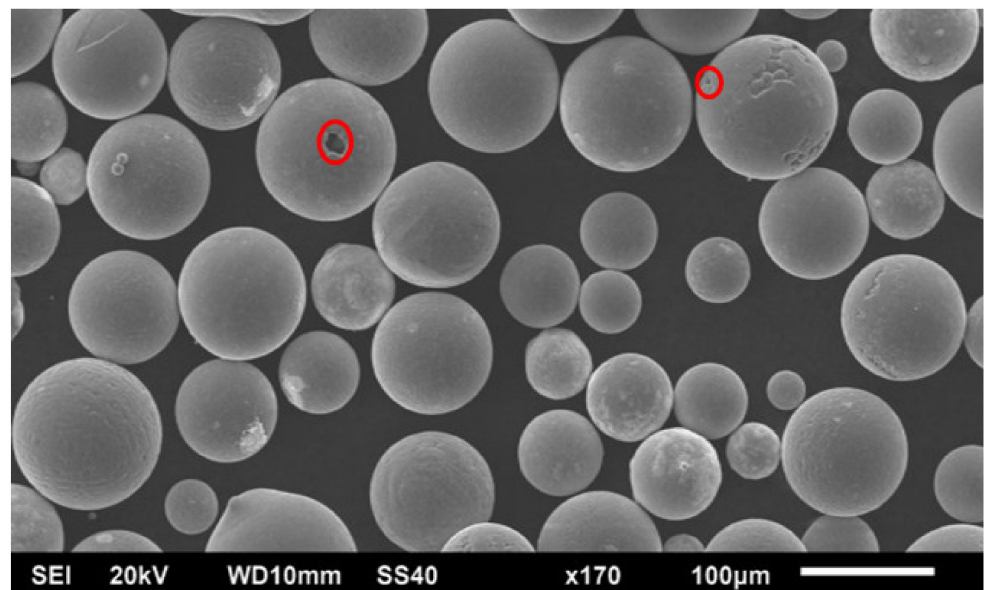


Figure 5. SEM secondary-electron image displaying an isolated pore on the surface of a particle circled in red.

3.3. PSD

The PSD is a measure of the frequency of various sized particles within a powder commonly represented by a cumulative frequency diagram or a histogram. The results from the laser diffraction measurements are given in Figure 6, in which the three tests represented by volume distribution are plotted. In Table 2, the average values of D_{10} , D_{50} and D_{90} are presented for all the three tests performed, with each D-value corresponding to the specified percentage of the powder that was less than or equal to a certain size. The three PSD curves overlap each other, implying that the size distributions of the samples spheroidised in the tests were similar.

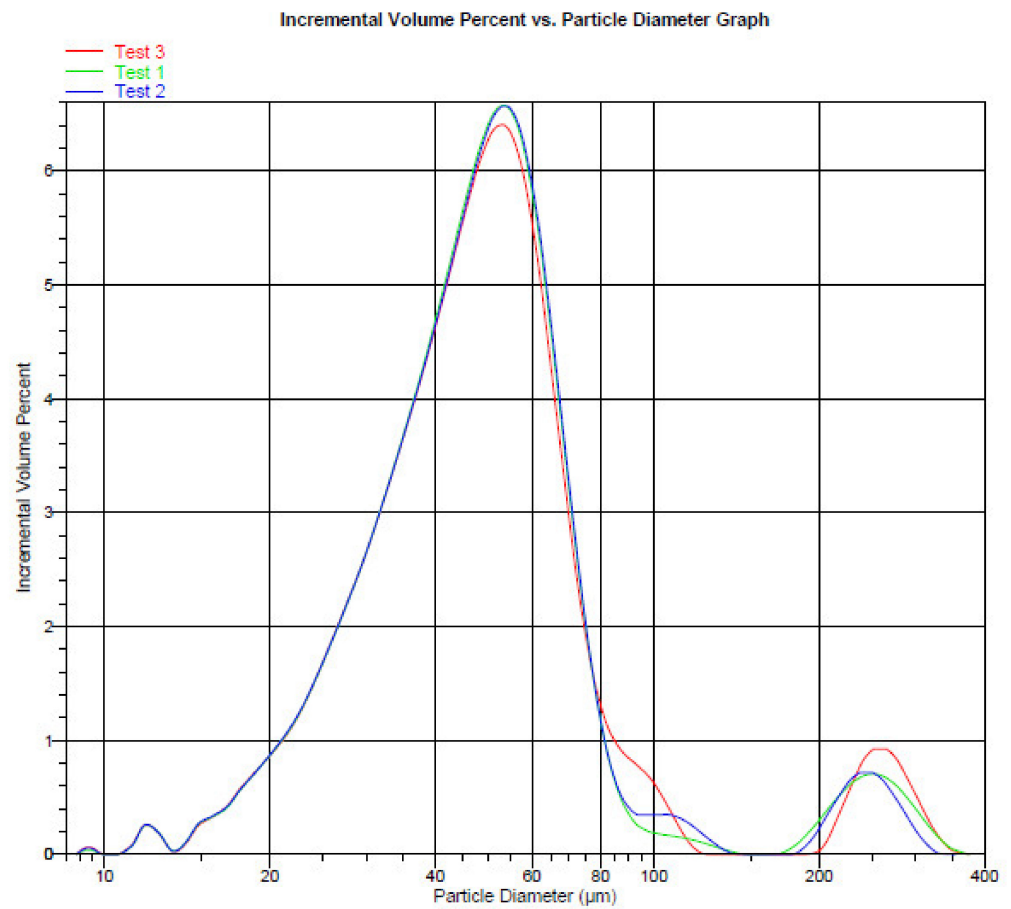


Figure 6. Incremental particle size distribution (PSD) curves for three spheroidised Ti6Al4V powder samples as determined with the laser diffraction technique.

Table 2. Numerical PSD results for the three spheroidised Ti6Al4V powder samples determined with the laser diffraction technique.

Group I	<20 µm	Not Recommended	3.2%
Group II	20–63 µm	Powder Bed Fusion	73.4%
Group III	63–150 µm	Direct Energy Deposition	18.3%
Group IV	>150 µm	Not Recommended	5.1%
D ₁₀	26.4 µm	/	/
D ₅₀	47.9 µm	/	/
D ₉₀	78.6 µm	/	/
Mean (µm)	58.8 µm	/	/
Median (µm)	47.9 µm	/	/

SEM was also used to quantitatively measure particle size, and this technique was treated as an alternative method to the laser diffraction PSD size distribution method. Subsequently, the particle size at the magnification of 500× was measured using a two dimensional approach, and the diameters of the particles were found to be between 66 µm and 98 µm, as shown in Figure 7.

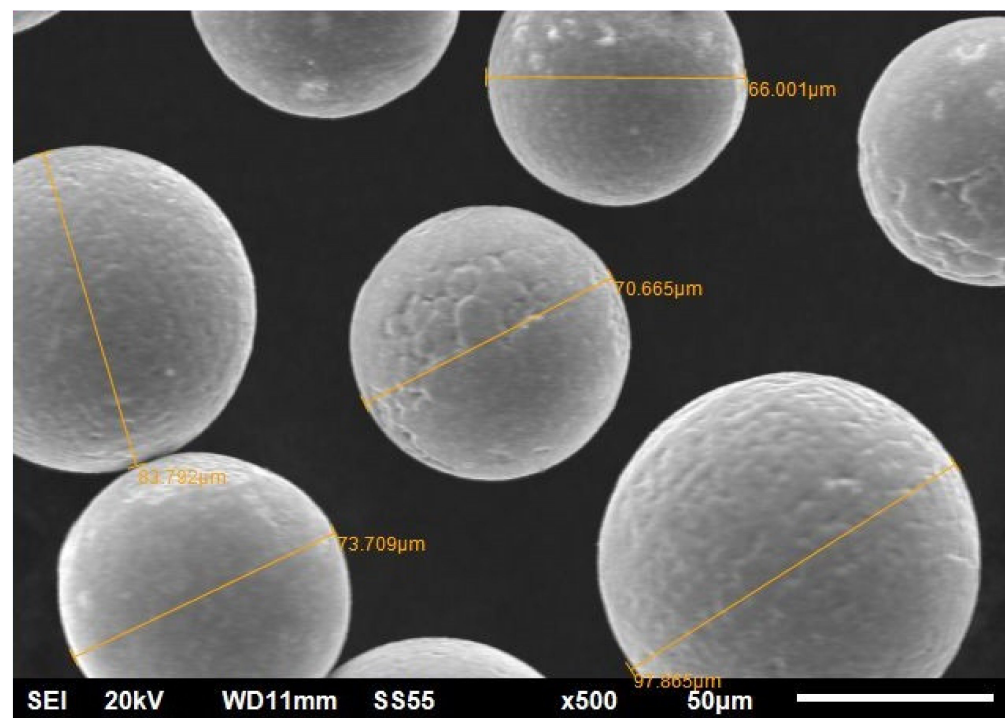


Figure 7. SEM secondary-electron image displaying the particle sizes of representative particles.

As discussed by Thejane et al. [26], the average D_{90} size of the Ti6Al4V commercial powder for DMLS is 35 μm , for LaserCusing powder it is 54 μm , and for the LENS powder it is 92 μm . The results presented in this paper indicated an average D_{90} size of 78.57 μm , which is a higher number than those of both DMLS and LaserCusing powders. This size distribution is not in the ideal range; however, it can be modified to the required range, depending on the feedstock. Sun et al. reported that a unique characteristic of PS is that the particle size of the feedstock does not change significantly during plasma processing [5]. On the other hand, Sheng et al. discovered that the average particle size could increase slightly and the size distribution could become narrower after PS [16]. Some melted small- or large-size powders may collide with each other and then grow up to a larger size particle. Therefore, the average size of powder increases, and the size distribution becomes narrower, after the plasma process. Additionally, these observations of larger-size particles suggested that large agglomerated particles melt to spherical powder due to limited coalescence and enough fusion temperature from plasma [16]. Therefore, through a combination of selecting an appropriate PSD of the feedstock powder and varying the plasma processing parameters, it should be possible to produce PSD ranges acceptable for various PBF systems.

3.4. Powder Composition

Some chemical variation can be expected between feedstock powder and produced components in any manufacturing process, but the chemical composition of the input material can provide an indication of whether the produced component will be suitable for the intended application. Figure 8 shows the areas, where EDS analyses were performed on powder particles with different surface features, and Table 3 shows the EDS elemental compositions of the spheroidised Ti6Al4V powders of both coarse and smooth surface features. From these results, it can be confirmed that Ti, Al and V were present in both the coarse and smooth particles of the spheroidised powder.

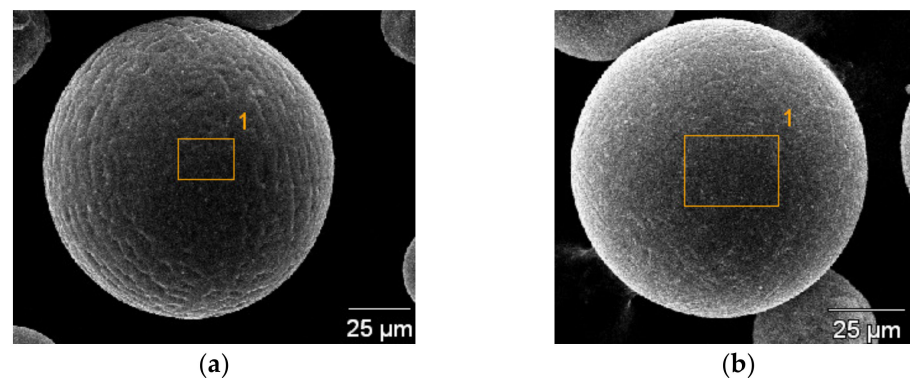


Figure 8. Areas where EDS analyses were performed on typical powder particles with coarse (a) and smooth (b) surface features.

Table 3. EDS elemental compositions of the spheroidised Ti6Al4V powders.

Element	Coarse Surface	Smooth Surface	ASTM F3001 Ti6Al4V (ELI)
Ti (wt %)	93.82	92.08	89
Al (wt %)	3.65	4.25	6.5–5.5
V (wt %)	2.53	3.68	3.5–4.5

ICP-OES is a trace-level elemental analysis technique that uses the emission spectra of a sample to identify and quantify the elements present. These results are more representative of the actual quantitative composition of the powder than the EDS results, which are from localized areas and are semi-quantitative. The typical ICP-OES results of the powder samples used in this study are given in Table 4, where a significant decrease of aluminium from the specified Ti6Al4V composition was observed. This result corresponds with the findings reported by Sun et al. [5]. They reported the loss of low-melting-point elements such as aluminium as a result of evaporation from the alloy due to the high plasma temperatures, as a potential issue of the PS process [5]. Thus, a further optimization of the process may be carried out to obtain a proper chemical composition of the resultant powder. Additional experimental work is still required to confirm whether powder of acceptable composition can be obtained.

Table 4. Inductively coupled plasma-optical emission spectroscopy (ICP-OES) chemical composition results.

Elements	Ti	Al	V	Fe
Spheroidised Ti6Al4V (wt %)	92.3	3.91	2.73	0.08
ASTM F3001 Ti6Al4V (ELI; wt %)	89	5.5–6.5	3.5–4.5	0.25

Tables 5 and 6 show the oxygen, nitrogen and hydrogen contents in the spheroidised powder as determined by an Eltra combustion analyser and the LECO ONH836 inert gas fusion analyser, respectively. The LECO ONH836 inert gas fusion analyser was found to be the more reliable analytical instrument than the Eltra combustion analyser because of its accuracy and low detection limits. Both the oxygen and hydrogen contents were above the ASTM specification, while the nitrogen content was just below the ASTM specification. The results obtained with the more reliable LECO ONH836 inert gas fusion analyser were closer to the ASTM standard specification as compared to the results obtained with the Eltra combustion analyser. The high oxygen content can be attributed to smaller particle sizes, as can be seen in Figures 3a and 5. These smaller particles had larger specific surface energies, thus resulting in a higher oxygen content. Therefore, to control the oxygen content of the spheroidised powder, it is necessary to control the PSD of the spheroidised powder.

Table 5. Results obtained with the Eltra combustion analyser.

Elements	Concentration
Oxygen	1.08%
Nitrogen	0.0905%

Table 6. Chemical content determined by the LECO ONH836 inert gas fusion analyser.

Sample	Oxygen (%)	Nitrogen (%)	Hydrogen (%)
Spheroidised Ti6Al4V powder	0.704	0.0486	0.068
ASTM F3001 Ti6Al4V (ELI)	0.13	0.05	0.012

4. Conclusions

The SEM micrographs confirmed that the particles of the spheroidised powder were spherical with no satellites, and from the PSD results, the particle size D_{10} was 26.4 μm and D_{90} was 78.6 μm . The chemical compositions of aluminum and vanadium were 3.91 wt % and 2.73 wt %, respectively, and they were out of specification. It is important to note that the oxygen and hydrogen contents of the spheroidised powder were higher than the one specified in the ASTM F3001 Ti6Al4V (ELI) standard. However, the iron chemical content was 0.08 wt %. From the results of this study, it can be concluded that when the spheroidisation process parameters of an ICP system are optimised for a particular powder feedstock consisting of irregular Ti6Al4V particles, particle morphology can be changed from irregular to spherical and PSD can be tailored to meet the requirements of a particular PBF system.

Author Contributions: Conceptualization, N.N., W.d.P. and H.B.; methodology, N.N.; validation, N.N., W.d.P. and H.B.; formal analysis, N.N.; writing—original draft preparation, N.N.; writing—review and editing, N.N., W.d.P. and H.B.; supervision, W.d.P. and H.B.; funding acquisition, W.d.P. and H.B. All authors have read and agreed to the published version of the manuscript.

Funding: The financial support of the South African Department of Science and Innovation (DSI) through the Nuclear Materials Development Network (NMDN) of the Advanced Materials Initiative (AMI) and Collaborative Program in Additive Manufacturing is gratefully acknowledged (Contract No. CSIR-NLC-CPAM-21-MOA-CUT-01).

Institutional Review Board Statement: Not applicable.

Informed Consent Statement: Not applicable.

Data Availability Statement: Not applicable.

Acknowledgments: The authors would like to acknowledge the Nuclear Materials Development Network (NMDN) of the Advanced Materials Initiative (AMI), funded by the Department of Science and Innovation (DSI) for the financial support in conducting this study. The South African Nuclear Energy Corporation (Necsa) is acknowledged for their financial support. The following Necsa personnel, i.e., M.M. and P.C.S., are thanked for their contributions of the plasma experiments.

Conflicts of Interest: The authors declare no conflict of interest.

References

1. *Mineral Commodity Summaries 2020*; US. Geological Survey: Reston, VA, USA, 2020; pp. 176–177. [[CrossRef](#)]
2. International Titanium Association. South Africa Moves Forward, Stakes Its Claim as Hub for Titanium Powder Metal Innovation. *Titan. Today* **2018**, *22*, 22–23.
3. Oosthuizen, S.J.; Swanepoel, J.J. Development status of the CSIR-Ti Process. *IOP Conf. Ser. Mater. Sci. Eng.* **2018**, *430*, 012008. [[CrossRef](#)]
4. Oliveira, J.P.; Lalonde, A.D.; Ma, J. Processing parameters in laser powder bed fusion metal additive manufacturing. *Mater. Des.* **2020**, *193*, 1–12. [[CrossRef](#)]

5. Sun, P.; Fang, Z.Z.; Zhang, Y.; Xia, Y. Review of the Methods for Production of Spherical Ti and Ti Alloy Powder. *J. Mater. Sci.* **2017**, *69*, 1853–1860. [[CrossRef](#)]
6. Oliveira, J.P.; Panton, B.; Zeng, Z.; Andrei, C.M.; Zhou, Y.; Miranda, R.M.; Fernandes, F.M.B. Laser joining of NiTi to Ti6Al4V using a Niobium interlayer. *Acta Materialia* Laser joining of NiTi to Ti6Al4V using a Niobium interlayer. *Acta Mater.* **2016**, *105*, 9–15. [[CrossRef](#)]
7. Callegari, B.; Oliveirac, J.P.; Aristizabal, K.; Coelho, R.S.; Brito, P.P.; Wug, L.; Schell, N.; Soldera, F.A.; Mücklich, F.; Pinto, H.C. Materials Characterization In-situ synchrotron radiation study of the aging response of Ti-6Al-4V alloy with different starting microstructures. *Mater. Charact.* **2020**, *165*, 1–10. [[CrossRef](#)]
8. Lisiecki, A.; Piwnik, J. Tribological characteristic of titanium alloy surface layers produced by diode laser gas nitriding. *Arch. Metall. Mater.* **2016**, *61*, 543–552. [[CrossRef](#)]
9. Gospodinov, D.; Ferdinandov, N.; Dimitrov, S. Classification, properties and application of titanium and its alloys. *Proc. Univ. Ruse* **2016**, *55*, 27–32.
10. Veiga, C.; Davim, J.P.; Loureiro, A. Properties and applications of titanium alloys: A brief review. *Rev. Adv. Mater. Sci.* **2012**, *32*, 14–34.
11. Elias, C.N.; Lima, J.H.C.; Valiev, R.; Meyers, M.A. Biomedical applications of titanium and its alloys. *JOM* **2008**, *60*, 46–49. [[CrossRef](#)]
12. Guo, J.; Fan, X.; Dolbec, R.; Xue, S.; Jurewicz, J.; Boulos, M. Development of nanopowder synthesis using induction plasma. *Plasma Sci. Technol.* **2010**, *12*, 188–199.
13. Vert, R.; Pontone, R.; Dolbec, R.; Dionne, L.; Boulos, M.I. Induction plasma technology applied to powder manufacturing: Example of Titanium-based materials. *Key Eng. Mater.* **2016**, *704*, 282–286. [[CrossRef](#)]
14. Zi, X.; Chen, C.; Wang, X.; Wang, P.; Zhang, X.; Zhou, K. Spheroidisation of tungsten powder by radio frequency plasma for selective laser melting. *Mater. Sci. Technol.* **2018**, *34*, 735–742. [[CrossRef](#)]
15. Bissett, H.; van der Wall, I.J. Metal and alloy spheroidisation for the Advanced Metals Initiative of South Africa, using high-temperature radio-frequency plasmas. *J. S. Afr. Inst. Min. Metall.* **2017**, *117*, 975–980. [[CrossRef](#)]
16. Sheng, Y.W.; Guo, Z.M.; Hao, J.J.; Yang, D.H. Effect of spheroidization of Ti-6Al-4V powder on characteristics and rheological behaviors of gelcasting slurry. *Procedia Eng.* **2012**, *36*, 299–306. [[CrossRef](#)]
17. Wei, W.; Wang, L.; Chen, T.; Duan, X.; Li, W. Study on the flow properties of Ti-6Al-4V powders prepared by radio-frequency plasma spheroidization. *Advance* **2017**, *28*, 2431–2437. [[CrossRef](#)]
18. Xie, B.; Fan, Y.; Zhao, S. Characterization of Ti6Al4V powders produced by different methods for selective laser melting. Characterization of Ti6Al4V powders produced by different methods for selective laser melting. *Mater. Res. Express* **2021**, *8*, 1–12. [[CrossRef](#)]
19. Li, J.; Hao, Z.; Shu, Y.; He, J. Fabrication of spherical Ti-6Al-4V powder for additive manufacturing by radio frequency plasma spheroidization and deoxidation using calcium. *J. Mater. Res. Technol.* **2020**, *9*, 14792–14798. [[CrossRef](#)]
20. Chong, Z.; Chaoyang, M.; Zicheng, W.; Yongge, C.; Ran, M.; Xuanyi, Y. Spheroidization of TC4 (Ti6Al4V) Alloy Powders by Radio Frequency Plasma Processing. *Rare Met. Mater. Eng.* **2019**, *48*, 2.
21. Yang, S.; Gwak, J.; Lim, T.; Kim, Y.; Yun, J. Preparation of Spherical Titanium Powders from Polygonal Titanium Hydride Powders by Radio Frequency Plasma Treatment. *Mater. Trans.* **2013**, *54*, 2313–2316. [[CrossRef](#)]
22. Daswa, P.; Gxowa, Z.; Monareng, M.; Mutombo, K. Effect of milling speed on the formation of Ti-6Al-4V via mechanical alloying. *IOP Conf. Ser. Mater. Sci. Eng.* **2018**, *430*, 1–5. [[CrossRef](#)]
23. Bissett, H.; van der Walt, I.J.; Havenga, J.L.; Nel, J.T. Titanium and zirconium metal powder spheroidization by thermal plasma processes. *J. S. Afr. Inst. Min. Metallurgy* **2015**, *115*, 937–942. [[CrossRef](#)]
24. *ASTM F3049-14 Standard Guide for Characterizing Properties of Metal Powders Used for Additive Manufacturing Processes*; ASTM International: West Conshohocken, PA, USA, 2014; pp. 1–3.
25. Li, Q.; Zhang, L.; Wei, D.; Ren, S.; Qu, X. Porous Nb-Ti based alloy produced from plasma spheroidized powder. *Results Phys.* **2017**, *7*, 1289–1298. [[CrossRef](#)]
26. Thejane, K.; Chikosha, S.; du Preez, W.B. Characterisation and monitoring of Ti6Al4V (ELI) powder used in different selective laser melting systems. *S. Afr. J. Ind. Eng.* **2017**, *28*, 161–171. [[CrossRef](#)]